ACS OMEGA

http://pubs.acs.org/journal/acsodf

Article

Biochemical Properties of β-Amylase from Red Algae and Improvement of Its Thermostability through Immobilization

Miyabi Murakami and Takashi Osanai*

Cite This: *ACS Omega* 2022, 7, 36195−36205

Read Online

ACCESS | Metrics & More | Article Recommendations | Supporting Information

ABSTRACT: β-Amylase hydrolyzes polysaccharides, such as starch, into maltose. It is used as an industrial enzyme in the production of food and pharmaceuticals. The eukaryotic red alga *Cyanidioschyzon merolae* is a unicellular alga that grows at an optimum pH of 2.0−3.0 and an optimum temperature of 40−50 °C. By focusing on the thermostability and acid resistance of the proteins of *C. merolae*, we investigated the properties of β-amylase from *C. merolae* (hereafter CmBAM) and explored the possibility of using CmBAM as an industrial enzyme. CmBAM showed the highest activity at 47 °C and pH 6.0. CmBAM had a relatively higher specificity for amylose as a substrate than for starch. Immobilization of CmBAM on a silica gel carrier improved storage stability and thermostability, allowing the enzyme to be reused. The optimum temperature and pH of CmBAM were comparable to those of existing β-amylases from barley and wheat. *C. merolae* does not use amylose, but CmBAM has a substrate specificity for both amylose and amylopectin but not for glycogen. Among the several β-amylases reported, CmBAM was unique, with a higher specificity for amylose than for starch. The high specificity of CmBAM for amylose suggests that isoamylase and pullulanase, which cleave the α-1,6 bonds of starch, may act together *in vivo*. Compared with several reported immobilized plant-derived β-amylases, immobilized CmBAM was comparable to β-amylase, with the highest reusability and the third-highest storage stability at 30 days of storage. In addition, immobilized CmBAM has improved thermostability by 15−20 °C, which can lead to wider applications and easier handling.

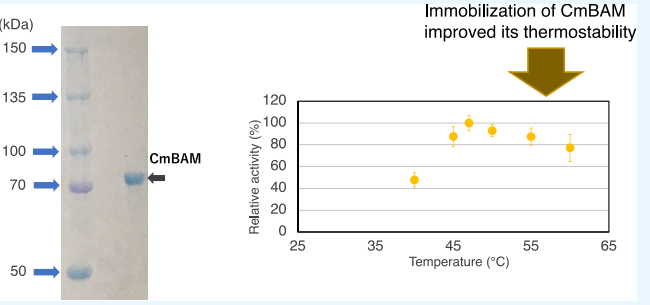

INTRODUCTION

Amylase accounts for 25−33% of the global enzyme market; has a wide range of applications, from food to brewing, pharmaceuticals, and textiles; and has been the subject of extensive research. Among the types of amylases, β-amylase (E.C. 3.2.1.2, α-1,4-D-glucan maltohydrolase) is an exo-type enzyme that hydrolyzes the α-1,4 linkage from the non-reducing end of the sugar chain to maltose units using polysaccharides such as starch as a substrate. β-Amylase is classified as a member of the glycosyl hydrolase, family 14.[1] β-Amylase alone cannot cleave the α-1,6 linkage and produce maltose and β-limit dextrin macromolecules; it promotes the hydrolysis of starch and amylopectin in combination with isoamylase (EC 3.2.1.68, glycogen α-1,6-glucanohydrolase) and pullulanase (EC 3.2.1.41, limit dextrinase, pullulan α-1,6-glucanohydrolase).[2,3] β-Amylase is an industrially important glycosidase that is used in the production of high-maltose syrup, food products as an antiaging agent for starchy foods, and infusions and glycosylation of pharmaceutical drugs.[2−4] Currently, most of the β-amylases used in the industry are derived from cereals such as barley and soybean, but the demand for cereals is increasing every year, and there are concerns about the stability of supply due to competition with their use in the food industry. Therefore, the searches for and studies of β-amylases from bacteria have been actively conducted, but few of them have been commercialized owing to the problems of yield, thermostability, and food safety.[5]

Immobilized enzymes are often ideal catalysts for the industry. Enzymes are usually solubilized, and problems exist such as the low stability to heat and pH and susceptibility to inhibition by substrates, products, metal ions, and chemicals.[6] The tolerance of metal ions is of particular importance in the enzyme application for its industrialization.[6] In addition, it is difficult and expensive to separate and recover the substrates and enzymes. Immobilization of enzymes, on the other hand, can improve their thermostability and stability, increase their activity, and enable their recovery and reuse, resulting in a cheaper cost of enzymes and expanded applications.[6−9] Among them, physical immobilization methods such as encapsulation, affinity ligands, and ionic and covalent bonding methods have

Received: May 27, 2022
Accepted: September 16, 2022
Published: October 3, 2022

been used.[10,11] Recently, cross-linked enzyme crystals and cross-linked enzyme aggregation have been reported.[12,13]

The eukaryotic red alga *Cyanidioschyzon merolae* is a unicellular alga that grows in environments with high temperatures of 40−50 °C, pH 2−3, around strongly acidic hot springs.[14,15] The complete genome of *C. merolae* has been sequenced.[15,16] As a model organism, the cell cycle, cell and organelle division,[16−18] genes related to oil and fat production, and environmental response mechanisms have been studied biochemically.[19−21] A few proteins that have been studied thus far in *C. merolae* are thermostable,[22,23] while more enzymes are expected to be thermostable. *C. merolae* has no cell wall, and intracellular components can be easily extracted using the osmotic shock method.[23] However, despite these advantages, there have been no studies on industrial enzyme production using *C. merolae*.

C. merolae uses UDP-glucose to synthesize floridean starch as a storage glucan, which accumulates as granular starch in the cytoplasm.[24] Floridean starch is composed of semiamylopectin, a polymer with a branching degree intermediate between amylopectin and glycogen.[25] *C. merolae* stores floridean starch, not triacylglycerol, as a major carbon storage during nitrogen starvation.[21] There are 30−40 enzymes related to starch synthesis and degradation in plants and green algae, with multiple gene duplications. In contrast, in *C. merolae*, there are only 11 enzymes related to starch synthesis and degradation.[26,27] Among the enzymes involved in glucan metabolism, there are two isoforms for the following two enzymes: 4-α-glucanotransferase (EC. 2.4.1.25, disproportionating enzymes, DPE1 or 2) and isoamylase, and *C. merolae* has minimal enzymes compared to higher plants and green algae.[28] In the starch hydrolysis pathway of *C. merolae*, two isoamylases and one pullulanase cleave the α-1,6 glycosidic linkages of glucans, whereas only one β-amylase hydrolyzes α-1,4 glycosidic linkages. These enzymes cannot directly cleave granular starch, but they phosphorylate and solubilize the surface of starch granules through glucan-water dikinase (GWD), leading to cleaving by various carbohydrate-hydrolyzing enzymes.[28] Maltose produced by the coupling of isoamylase, pullulanase, and β-amylase is metabolized by 4-α-glucanotransferase (DPE2).[26,29] β-Amylases are widely distributed among both prokaryote and eukaryote, and the catalytic domain, consisting of two glutamate residues and a flexible loop, is identified.[5] In the model presented by Ball et al. (2011), glycogen phosphorylase (EC 2.4.1.1) also contributes to the degradation of maltooligosaccharides.[26] In spite of these models, the kinetic parameters in these enzymes remain to be determined quantitatively.

In this study, we clarified the properties of *C. merolae* β-amylase (CmBAM) and compared these with those of existing enzymes, revealing the metal tolerance of CmBAM. We also improved the reusability and stability of CmBAM by immobilizing CmBAM on a silica-based porous carrier to produce a nanobiocatalyst with superior biochemical features over known β-amylases.

MATERIALS AND METHODS

Preparation of an Expression Vector Containing CmBAM. The genomic region contains CmBAM (CMJ087C) with an N-terminal *Bam*HI and a C-terminal *Xho*I fragment, and cloning of the DNA fragment into the *Bam*HI-*Xho*I site of the pGEX6P-1 vector (GE Healthcare, Little Chalfont, United Kingdom) was performed by Eurofins Genomics Japan (Tokyo, Japan). Codon usage was optimized for *Escherichia coli*.

Expression and Purification of Recombinant CmBAM. A vector containing the CmBAM artificial gene tagged with glutathione-*S*-transferase (GST) generated by Eurofins Genomics Japan was transformed into *E. coli* BL21 (DE3) competent cells (Biodynamics Research Institute, Inc., Tokyo). *E. coli* BL21 (DE3) was cultured with several liters of the LB medium (Becton, Dickinson and Company, Franklin Lakes, NJ) at 30 °C overnight with shaking at 150 rpm, and 0.01 mM isopropyl β-D-1-thiogalactopyranoside (Wako Chemical, Osaka, Japan) was added to the culture medium to induce the expression of GST-tagged CmBAM. The expressed GST-tagged CmBAM protein was purified by affinity chromatography, with some modifications.[22] The *E. coli* culture medium (4 L) was collected by repeated centrifugation (5800*g*, 2 min, 25 °C) and added to approximately 35 mL of 1× PBS-T (0.14 M NaCl, 2.7 mM KCl, 8.1 mM $Na_2HPO_4{\cdot}12H_2O$, 1.5 mM KH_2PO_4, 0.05% Tween-20) with cOmplete Mini protease inhibitor cocktail 1/5 tablets. The collected *E. coli* cells were sonicated 10 times for 20 s each time with 20% amplitude to disrupt the cells and elute GST-tagged CmBAM into the soluble fraction (VC-750, EYELA, Tokyo, Japan). Insoluble fractions such as cells were removed by centrifugation at 14,160*g* for 15 min at 4 °C, and 1 mL of Glutathione Sepharose 4 B Resin (GE Healthcare Japan, Tokyo, Japan) was added to the soluble fraction containing GST-tagged CmBAM. The mixture was shaken on ice for 1 h to bind GST-tagged CmBAM to glutathione Sepharose 4 B resin. After centrifugation to remove the supernatant, 3 mL or 500 μL of PBS-T was added and centrifuged (5800*g*, 2 min, 25 °C) to remove foreign substances, and the resin was washed five times. Next, 500 μL of GST elution buffer (50 mM Tris−HCl, pH 8.0, 10 mM reduced glutathione) was added to the resin, and GST-tagged CmBAM was eluted five times and concentrated using a VivaSpin 500 MWCO 50,000 instrument (Sartorius, Göttingen, Germany). Protein purification of the GST-tagged CmBAM was confirmed by SDS-PAGE, and the protein concentration was calculated using the Pierce BCA Protein Assay kit (Thermo Scientific, Rockford, IL).

***C. merolae* Strain and Culture Conditions.** *C. merolae* NIES-3377 obtained from the National Institute for Environmental Sciences (Tsukuba, Japan) was cultured, and the collected cells were used for the extraction of crude CmBAM. *C. merolae* was cultured in light with an intensity of 120 μmol photons m^{-2} s^{-1} with aeration of 1% (v/v) CO_2 at 40 °C and pH 2.5.*C. merolae* was cultured in 70 mL of the M-Allen medium (https://mcc.nies.go.jp/medium/ja/m_allen.pdf, National Institute for Environmental Studies, Tsukuba, Japan) starting at OD_{730} = 0.4 for 3 days. Cell densities were measured at OD_{730} using a Shimadzu UV-2400 spectrophotometer (Shimadzu, Kyoto, Japan).

Extraction of Crude β-Amylase from *C. merolae* or Malt Flour. Extraction aliquots (5 mL) contained 0.5 g malt flour or 7.06 mg CDW (cell dry weight)/mL of *C. merolae* cells in 50 mM Tris−HCl buffer (pH 8.0), 1 mM EDTA, 0.001% sodium azide, and 100 mM cysteine. The solutions were sonicated for 200 s at 20% intensity (VC-750, EYELA, Tokyo, Japan). The mixture was agitated with a vortex mixer for 10 s every 10 min while shaking for 1 h at room temperature (24−26 °C) and then centrifuged (5800*g*, 10 min, 25 °C), and the supernatant was collected. The crude β-amylase extracts were appropriately diluted with MES buffer (100 mM, pH 6.2)

https://doi.org/10.1021/acsomega.2c03315
ACS Omega 2022, 7, 36195−36205

containing 1 mM EDTA and 1 mg/mL BSA to a suitable concentration for the Betamyl-3 assay.

Enzyme Assays for Recombinant CmBAM. The CmBAM activity was determined by measuring the reducing sugar amounts produced by the enzyme reaction using the dinitrosalicylic acid (DNS) method[30] with some modifications. The assay aliquot (400 μL) contained 50 mM citrate buffer (pH 6.0), 27.5 nM free GST-tagged CmBAM, and various concentrations of soluble starch (0.063−2%) (Wako, Osaka, Japan), 0.5% amylose, 0.5% amylopectin, or 0.5% glycogen. Before the addition of substrates, the assay solution of CmBAM was incubated at 47 °C for 1 min. Thereafter, soluble starch was added to the assay solution to initiate the reaction. After incubation of the solution at 47 °C for 10 min, the reaction was terminated by the addition of 400 μL of 3,5-dinitrosalicylic acid reagent and boiling the solution for 5 min. The activity of CmBAM was calculated by monitoring the absorbance at A_{540} using a Shimadzu UV-1850 (Shimadzu, Kyoto, Japan) and measuring the amount of maltose as a reducing sugar. The amount of liberated maltose was calculated from the maltose standard curve. All assays were repeated three times. One unit (U) of β-amylase activity was defined as the amount of enzyme necessary to produce 1 μmol of maltose per minute under optimum conditions. The maximum reaction velocity (V_{max}), turnover number (k_{cat}), and Michaelis constant (K_m) (substrate concentration at 50% V_{max}) of CmBAM for soluble starch were calculated by curve fitting of the Michaelis−Menten equation using KaleidaGraph ver. 4.5. The data used for kinetic analysis in Table 1 are shown in Figure S1.

Table 1. K_m Values and k_{cat} for Soluble Starch of β-Amylases from Various Organisms[a]

organism	K_m (mg/mL)	k_{cat} (s^{-1})	reference
Cyanidioschyzon merolae	4.0	3200	
rice (*Oryza sativa*)	3.0		45
soybean (*Glycine max*)	1.9	1280	46
Medicago sativa (light or heavy)	5.9 or 6.8		47
Abrus precatorius	79.4		35
Clostridium thermosulphurogenes	1.7	7333	36
Bacillus cereus	0.7	2739	48

[a] β-Amylases from plants or bacteria were selected for comparison. K_m values are represented as the concentration of starch in mg/mL. In the report of Doehlert et al., light indicates β-amylase with a molecular weight (MW) of 41,700 and heavy indicates a MW of 65,700.[45]

Determination of Optimum pH and Temperature of CmBAM. CmBAM activity was determined using a pH range of 3−10 at 40 °C in the following buffers: 50 mM citrate buffer (pH 3−8), 50 mM sodium phosphate buffer (pH 6 or 7), 50 mM glycine-HCl buffer (pH 2 or 3), or 50 mM glycine-NaOH buffer (pH 8−10). Thereafter, the optimal temperature was determined by incubation at temperatures between 30 and 60 °C with 50 mM citrate buffer (pH 6.0).

Effects of Metal Ions or Chemical Reagents on CmBAM Activity and Stability. CmBAM activity with metal ions or compatible solutes was measured under optimal assay conditions and represented as a relative activity to the activity without additives that was 100%. The following reagents were added: 1 or 10 mM $FeCl_2$, $ZnSO_4$, $CuSO_4$, $Co(NO_3)_2$, NaCl, $NaNO_3$, KCl, KNO_3, $CaCl_2$, $MgCl_2$, $MgSO_4$, betaine (*N*,*N*,*N*-trimethylglycine), and trehalose and 0.5 mM maltose.

Enzyme Assays of Crude β-Amylases from *C. merolae* Cells and Malt Flour Using the Betamyl-3 Kit. Crude CmBAM and malt β-amylase levels were determined using the Betamyl-3 kit (Megazyme International, Ireland). Crude β-amylase activity was measured using the substrate *p*-nitrophenyl-β-D-maltotriose (PNPβ-G3). Aliquots (1.7 mL) contained the extracted solutions of CmBAM or malt β-amylase, Betamyl-3 reagent, and 1 M Tris−HCl buffer (pH 8.5). Before adding substrates, the assay solution of CmBAM and malt β-amylase was incubated for 5 min at 40 °C. Thereafter, 0.1 mL of the Betamyl-3 reagent was added to the assay solution to start the reaction. After incubation at 40 °C for 10 min, 1.5 mL of 1 M Tris HCl buffer (pH 8.5) was added to the reaction mixture to stop the reaction. The activities of CmBAM and malt β-amylase were calculated by absorbance at A_{400} using a Shimadzu UV-1850 (Shimadzu, Kyoto, Japan). The activity of the enzyme was defined as 1 Betamyl-3 unit, which is the amount of β-amylase enzyme required to produce 1 μmol of *p*-nitrophenol per min from PNPβ-G3 by the coupling reaction of β-amylase and thermostable β-glucosidase under the conditions described above.

CmBAM Immobilization. The carrier used for immobilization was an aminosilane-treated silica gel carrier (Oji Scientific Instruments, Tokyo, Japan). The carrier (5−160 mg) and 5% glutaraldehyde (2 mL) were added to a 20 mL glass bottle. To remove air from the micropores of the carrier, it was placed in a vacuum aspirator for 15 min at reduced pressure and 45 min at ambient pressure. After 45 min of standing, it was washed three times with water. We also performed this immobilization with different silica gel amounts (Figure S3A) and mixing the enzymes and silica gel with rotary stirring (Figure S3B), but similar results were obtained. Glutaraldehyde was then removed by replacing it with 2 mL of 100 mM sodium phosphate buffer. Formylation was complete up to this point. Then, 1−100 μg of CmBAM solution and several milliliters of 100 mM sodium phosphate buffer were added to make the total volume 2 mL, and the pressure was reduced again for 15 min. The enzyme was then adsorbed onto the carrier by incubating at 4 °C for 12 h. The immobilization efficiency of CmBAM was calculated from the amount of protein and the activity ratio. The amount of protein was calculated by measuring the amount of CmBAM protein remaining in the immobilized supernatant without being adsorbed onto the carrier. The free CmBAM concentration was calculated using a Pierce BCA Protein Assay kit (Thermo Scientific, Rockford, IL, USA). The calculation method based on the activity ratio of immobilized and free enzymes was based on the following formula:[7]

$$\text{Immobilization efficiency}(\%) = \frac{\text{specific activity of immobilized CmBAM(U)}}{\text{specific activity of free CmBAM(U)}} \times 100$$

Thermostability Measurements of Free or Immobilized CmBAM. Thermostability was determined by measuring the residual activity of free or immobilized CmBAM after preincubation for 30 min at different temperatures (30−70 °C) with no reagent, 10 mM betaine, 10 mM $CaCl_2$, or 1 mM maltose. Free or immobilized CmBAM activities were represented as residual activities, and the activity without heat treatment was set at 100%.

https://doi.org/10.1021/acsomega.2c03315
ACS Omega 2022, 7, 36195−36205

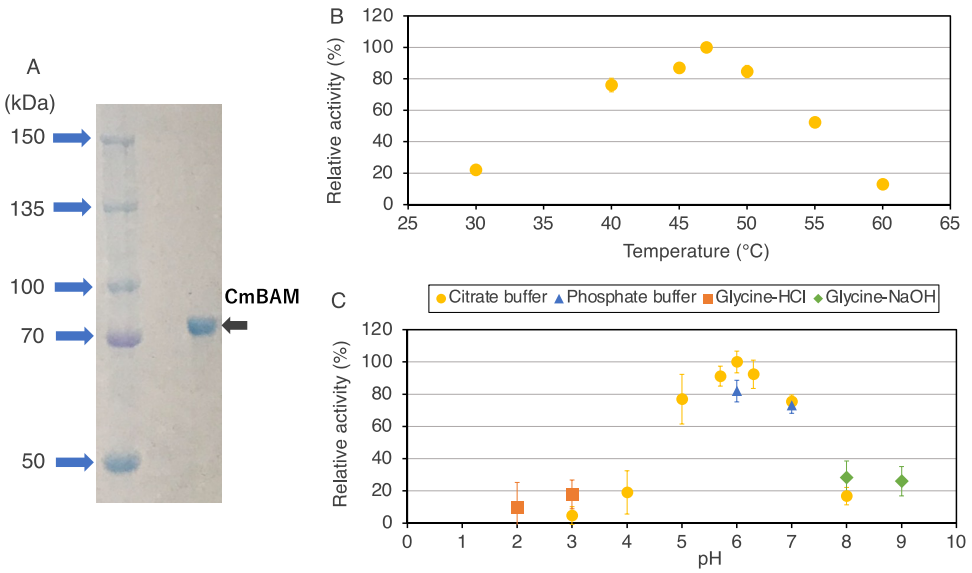

Figure 1. (A) Purification of GST-tagged CmBAM. SDS-PAGE gels (8%) were stained with InstantBlue (Expedeon Protein Solutions, San Diego, CA). The molecular weight marker used was Precision Plus Protein Dual Color Standard (Bio-Rad Laboratories, Hercules, CA), and each molecular weight was noted. Photograph courtesy of Miyabi Murakami. Copyright 2022. (B) CmBAM activity at each temperature. The activity of CmBAM was represented as a relative activity with the activity at 47 °C as 100%. Measurement was performed using 50 mM sodium citrate buffer (pH 6.0). The soluble starch concentration was 0.5% w/v. (C) CmBAM activity using various buffers at each pH. Yellow dots, blue triangles, orange squares, and green rhombuses represent 50 mM sodium citrate buffer, 50 mM sodium phosphate buffer, 50 mM glycine-HCl buffer, and 50 mM glycine-NaOH buffer, respectively. The activity of CmBAM was represented as a relative activity with the activity in 50 mM sodium citrate buffer (pH 6.0) as 100%. The measurements were performed at 40 °C. The soluble starch concentration was 0.5% w/v. All data of (B) and (C) represent the means ± SD from three independent experiments.

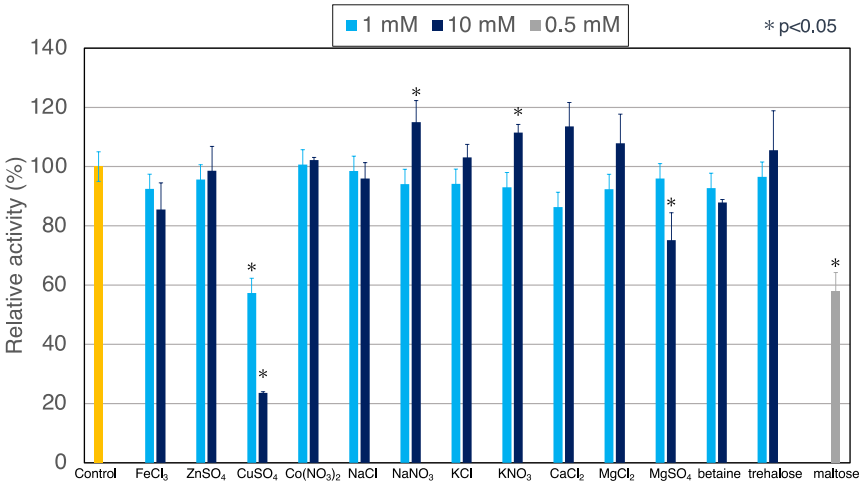

Figure 2. Effects of various metal ions and some compatible solutes on CmBAM activity using 0.5% soluble starch as a substrate. CmBAM activity was measured using various compatible solutes or metal ions under optimum conditions (pH 6.0 sodium citrate buffer, 47 °C). The yellow bar represents control data. Light blue, navy blue, and gray bars represent concentrations of 1, 10, and 0.5 mM metal ions or compatible solutes, respectively. The data represent the means ± SD from three independent experiments. Asterisks (*) indicate a significance level of $P < 0.05$ based on statistical analysis by Student's *t*-test.

Storage Stability of Free or Immobilized CmBAM. The storage stability of free and immobilized CmBAM was determined at different times (1−30 days). Residual CmBAM activity was calculated as a percentage of the initial CmBAM activity. The free or immobilized CmBAM activities were represented as residual activities, and the initial activity of CmBAM was set at 100%.

Reusability of Immobilized CmBAM. The reusability of the immobilized CmBAM was evaluated by repeated use for 10 cycles. One cycle refers to the reaction of immobilized CmBAM for 10 min under optimal conditions, and then the immobilized CmBAM and the product were separated. For each assay, immobilized CmBAM was left on ice for 10 min. The residual activity after repeated use was represented as the fraction of the initial activity that was set as 100%.

Sequence Alignment and Phylogenetic Analysis. Sequences of 20 β-amylases were obtained from GenBank. The β-amylase sequence alignment was performed using CLC Sequence Viewer ver. 7.0. PhyML online (http://www.atgc-montpellier.fr/phyml/) was used to generate phylogenetic trees using the maximum likelihood method. The 3D modeling

https://doi.org/10.1021/acsomega.2c03315
ACS Omega 2022, 7, 36195−36205

of CmBAM was performed with its sequence at the SWISS-MODEL server (https://swissmodel.expasy.org).

RESULTS

Biochemical Properties of CmBAM. Glutathione-*S*-transferase (GST)-tagged CmBAM was expressed in *E. coli* BL21 and purified by affinity chromatography. GST-tagged CmBAM proteins (84.5 kDa) were obtained and verified by SDS-PAGE (Figure 1A). First, the result of the assay by the Betamyl-3 kit showed that the obtained enzyme had activity as *β*-amylase. CmBAM showed the highest activity at 47 °C in 50 mM sodium citrate buffer (pH 6.0) (Figure 1B). In addition, CmBAM showed the highest activity at pH 6.0 in sodium citrate buffer (Figure 1C). The CmBAM activity in citrate buffer (pH 6.0) was set as 100%, and the relative activity of CmBAM at each pH and each buffer was expressed (Figure 1C). We performed a similar experiment using CmBAM without GST-tag, but the enzymatic activities were similar irrespective of GST-tag (Figure S2), and thus, subsequent experiments were performed with GST-tagged CmBAM. The kinetic parameters for soluble starch were then calculated; V_{max} was 284 U/mg, K_m was 4.0 ± 0.4 mg/mL, k_{cat} was 3200 ± 43.2 s^{-1} (Table 1), and k_{cat}/K_m was 792 ± 10.6 mL mg^{-1} s^{-1}.

Effect of Additive Metal Ions and Compatible Solutes. We investigated the changes in activity by adding various metal ions and cations, sugars, and glycine betaine, a known compatible solute. $NaNO_3$ (10 mM) and KNO_3 (10 mM) increased the CmBAM activity by 15.0 and 11.4%, respectively (Figure 2). In contrast, 1 and 10 mM $CuSO_4$ decreased the CmBAM activity by 42.7 and 76.4%, 10 mM $MgSO_4$ by 24.8%, 10 mM betaine by 12.1%, and 0.5 mM maltose by 42% (Figure 2). All additives of 1 mM except for $CuSO_4$ had few effects. In addition, 10 mM $FeCl_3$ decreased the CmBAM activity by 14.5%; $ZnSO_4$, NaCl, KCl, $CaCl_2$, $MgCl_2$, and trehalose slightly increased or decreased the activity, but no significant difference was observed (Figure 2).

Thermostability of CmBAM. Next, we examined the thermostability of the CmBAM. The activity of CmBAM decreased to 83.4% at 40 °C, 59.8% at 50 °C, and 6.8% at 60 °C, and almost no activity was observed at 70 °C after incubation for 30 min at each temperature (Figure 3). Furthermore, 1 mM betaine, 10 mM $CaCl_2$, or 1 mM maltose was added; the enzyme was incubated at the above temperatures for 30 min; and the activity was measured at 47 °C. After adding 10 mM betaine, the residual activity of CmBAM remained at 89.1% at 40 °C, 82.6% at 50 °C, 9.7% at 60 °C, and 5.7% at 70 °C (Figure 3). After adding 10 mM $CaCl_2$, the activity was 90.6% at 30 °C, 83.3% at 40 °C, 49.2% at 50 °C, and 2.2% at 60 °C, and there was almost no activity at 70 °C incubation (Figure 3). With the addition of 1 mM maltose, the residual activity of CmBAM remained at 92.7% at 40 °C, 61.6% at 50 °C, and 1.1% at 60 °C incubation (Figure 3).

Specificity for Various Substrates. The substrate specificity of CmBAM using amylose, amylopectin, or glycogen as substrates was 122, 71, and 1.4%, respectively, while the activity of CmBAM using soluble starch was 100% (Table 2). The affinity of CmBAM using glycogen was lower than that of other substrates (Table 2).

Immobilization of CmBAM. The immobilization efficiency of CmBAM was 32.9 ± 8.4% of the activity ratio (Figure 4A). After immobilization by adding 550 nM of CmBAM, the amount of CmBAM remaining in the supernatant solution was 360.8 ± 27.5 nM (Figure 4B). Calculated from the theoretical amount of immobilized enzyme, the reaction of 27.5 nM of the enzyme showed the same activity as the free enzyme. The optimum temperature and pH of CmBAM did not change before and after immobilization (Figure 4C,D), while the activity of immobilized CmBAM was 8% higher at 50 °C, 35% higher at 55 °C, and 64% higher at 60 °C than that of free CmBAM (Figure 4C). The thermostability of the immobilized enzyme was 91.2, 91.7, and 46.6% at 50, 60, and 70 °C, respectively (Figure 5). In addition, the enzyme was refrigerated at 4 °C for 2 weeks. As a result, 95.2% of the activity of free CmBAM remained after 7 days, 92.2% after 10 days, 89.9% after 14 days, and 71.6% after 30 days of storage, while the immobilized CmBAM maintained its activity after 1−3 days, 93.4% after 7 days, 87.1% after 10 days, 86.7% after 14 days, and 82.1% after 30 days of storage (Figure 6A). After 10 uses, 81.2% of the activity remained (Figure 6B).

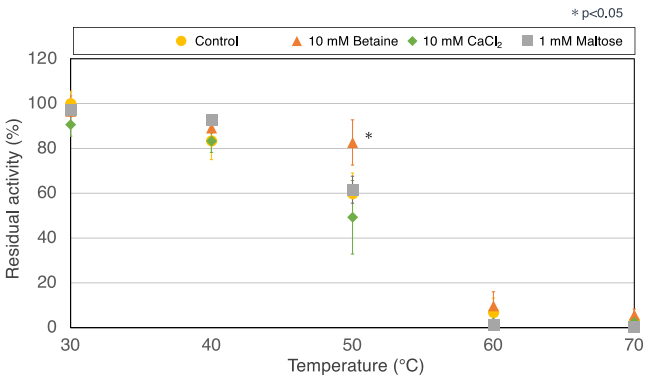

Figure 3. Thermostability of CmBAM. The residual activities of CmBAM were measured after heat treatment at each temperature for 30 min. Measurements were performed in 50 mM sodium citrate buffer (pH 6.0) after heat treatment. Yellow dots represent control data. Orange triangles, green rhombuses, and gray squares represent heat treatment after adding 10 mM betaine, 10 mM $CaCl_2$, or 1 mM maltose, respectively. All the enzymatic activities are represented by residual activities, and the activity without heat treatment was set at 100%. The data represent the means ± SD from three independent experiments. An asterisk (*) indicates a significance level of $P < 0.05$ based on statistical analysis by Student's *t*-test.

Comparison of the Activity of Crude Enzymes Extracted from *C. merolae* Cells or Malt Flour. Since all experiments in this study were performed using recombinant CmBAM, we extracted crude CmBAM from *C. merolae* cells and measured the activity of crude CmBAM using a Betamyl-3 kit to confirm the actual expression and activity of CmBAM *in vivo*. The crude CmBAM showed an activity of 21.7 U/g cell dry weight (CDW).

Sequence Alignment and Phylogenetic Analysis Revealed the Distinct Cluster of CmBAM from Plant and Bacteria. We compared the amino acid sequences of *β*-amylase from eukaryotic red algae, green algae, higher plants, and bacteria and performed phylogenetic analysis (Figures 7 and 8). The glutamate residues at positions 239, 409, and 443 corresponding to CmBAM are essential for catalysis (Figure 7 and Figure S4). The flexible loop consisting of residues at positions 102−109 holds the sugar chain in the catalytic position[33] (Figure 7). The aspartic acid residue at position 107 on the flexible loop is an important residue that forms a hydrogen bond with the sugar chain. In addition, cysteine residues at positions 101, 407, and 261 are involved in the

https://doi.org/10.1021/acsomega.2c03315
ACS Omega 2022, 7, 36195−36205

Table 2. Activity of β-Amylases Derived from Various Sources Using Various Substrates[a]

	Cyanidioschyzon merolae	*Bacillus flexus*	*Clostridium thermosulphurogenes*	barley (*Hordeum vulgare*)	wheat (*Triticum aestivum*)	soybean (*Glycine max*)
soluble starch	100	100	100	100	100	100
amylose	122	98	129	72	67	85
amylopectin	71	83	112	72	74	71
glycogen	1.4	51	150	0.8	0.5	1

[a]The activity for each substrate was expressed as a relative activity when the activity for soluble starch as a substrate was set to 100%. Data for *B. frexus*, barley, wheat, and soybean were taken from the study by Sugita et al. (2011).[5] *C. thermosulphurogenes* data were obtained from the study of Shen et al. (1988).[37]

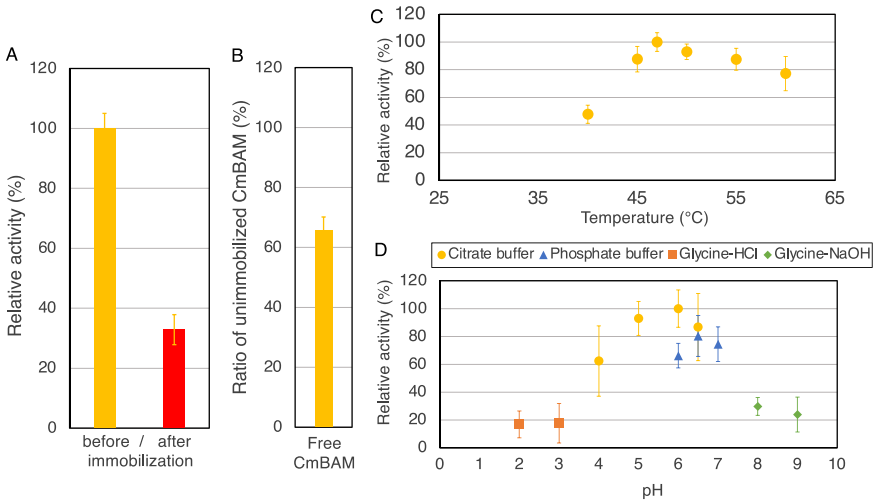

Figure 4. Immobilization of CmBAM. (A) Immobilization efficiency of CmBAM. The yellow bar represents the activity of 27.5 nM free CmBAM before immobilization. The red bar represents the relative activity of CmBAM after immobilization, and the activity of free CmBAM before immobilization was set at 100%. The red bar shows the immobilization rate as an activity ratio when 27.5 nM CmBAM is added in immobilization process. The data represent the means ± SD from three independent experiments. (B) Remaining ratio of unimmobilized CmBAM protein in the supernatant. The ratio of unimmobilized CmBAM protein that remained in the supernatant after immobilization process is expressed as a percentage. The 550 nM CmBAM added for the immobilization process was set at 100%. (C) Immobilized CmBAM activity at each temperature. Yellow dots, blue triangles, orange squares, and green rhombuses represent 50 mM sodium citrate buffer, 50 mM sodium phosphate buffer, 50 mM glycine-HCl buffer, and 50 mM glycine-NaOH buffer, respectively. The activity of CmBAM was represented as a relative activity with the activity at 47 °C as 100%. Measurement was performed using 50 mM sodium citrate buffer (pH 6.0). The soluble starch concentration was 0.5% w/v. (D) CmBAM activity using various buffers at each pH. The activity of CmBAM was represented as a relative activity with the activity in 50 mM sodium citrate buffer (pH 6.0) as 100%. The measurements were performed at 47 °C. The soluble starch concentration as substrate was 0.5% w/v. The data represent means ± SD from three independent experiments.

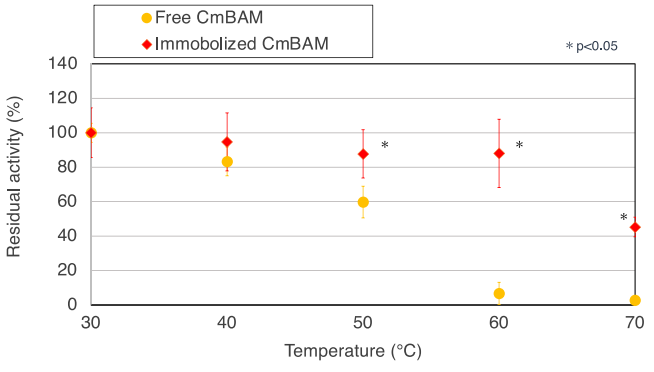

Figure 5. Thermostability of immobilized CmBAM. The residual activities of CmBAM were measured after heat treatment at each temperature for 30 min. Measurements were performed using 50 mM sodium citrate buffer (pH 6.0). Red rhombuses represent the relative activity of immobilized CmBAM, and the activity without heat treatment was set at 100%. Control data of yellow dots are the same data as those in Figure 3. The data represent the means ± SD from three independent experiments. Asterisks (*) indicate a significance level of $P < 0.05$ based on statistical analysis by Student's *t*-test.

action of the SH reagent (the cysteine residue at position 261 is conserved only in β-amylase from plants) (Figure 7). CmBAM possesses a characteristic inserted region at positions 156 to 199 (Figure 7 and Figure S4).

DISCUSSION

The optimum pH of CmBAM was 6.0, which is consistent with the fact that the intracellular pH of *C. merolae* is maintained between 6.3 and 7.1 and the extracellular pH is between 1.5 and 7.5,[32] indicating that CmBAM is an enzyme that functions intracellularly in *C. merolae*. The optimal temperature of CmBAM was similar to that of β-amylase from barley and wheat but not similar to that of β-amylase from soybean or bacteria (Table 3). The thermostability of CmBAM was similar to that of β-amylase from barley. β-Amylase from soybean and *Bacillus* sp. showed higher thermostability than CmBAM, maintaining 85−90% of its activity even after treatment at 60 °C (Table 4).

Kaplan et al. reported that maltose protects intracellular proteins and acts as a compatible solute against cold, hot, or osmotic stresses in *Arabidopsis thaliana*.[33] Betaine increased the residual activity of CmBAM at 50 °C by 20%, but 1 mM

https://doi.org/10.1021/acsomega.2c03315
ACS Omega 2022, 7, 36195−36205

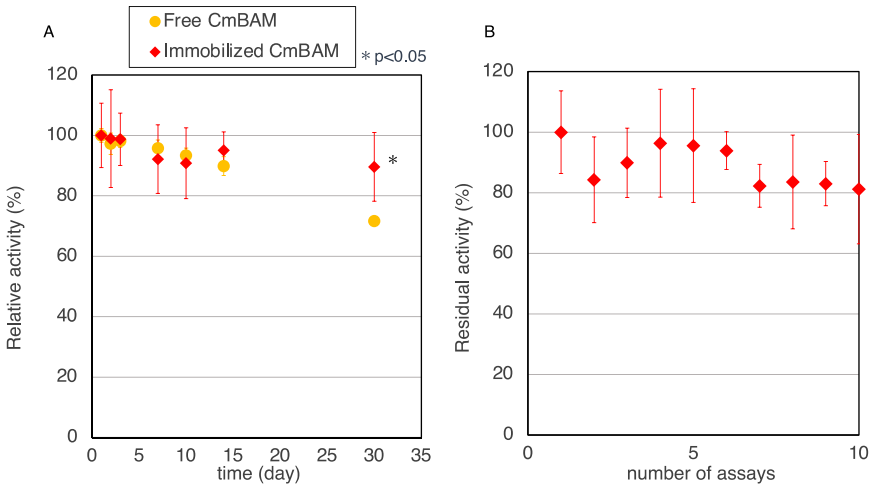

Figure 6. (A) Storage stability of free or immobilized CmBAM. The storage stability of free or immobilized CmBAM stored at 4 °C in 50 mM sodium phosphate buffer (pH 7.0). The protein concentrations of free or immobilized CmBAM are 550 nM in 200 μL buffer or 1 μg/4 mg carrier in 100 μL buffer, respectively. Yellow dots and red rhombuses represent the relative activity of free or immobilized CmBAM, respectively, and the activity of day 1 (not stored) was set at 100%. An asterisk (*) indicates a significance level of $P < 0.05$ based on statistical analysis by Student's *t*-test. (B) Reusability of immobilized CmBAM (10 times). The measurements of CmBAM activity, after being stored and reused each time, were performed at 47 °C using 50 mM sodium citrate buffer (pH 6.0). The soluble starch concentration was 0.5% w/v. The data represent the means ± SD from three independent experiments.

Table 3. Optimum pH and Temperature for the Activity of β-Amylase from Various Organisms[a]

organism	optimum pH	optimum temperature (°C)	reference
Cyanidioschyzon merolae	6	47	
barley (*Hordeum vulgare*)	4.8−5.0	55	49
soybean (*Glycine max*)	5.4	60	49
wheat (*Triticum aestivum*)	4.5−6.5	40	50
Bacillus cereus	7−8	37−50	51
Bacillus megaterium	7.5	60	52
Bacillus flexus	8	55	5

[a]β-Amylases from plants or bacteria were selected for comparison.

Table 4. Thermostability of β-Amylase from Various Organisms[a]

organism	50 °C	60 °C
Cyanidioschyzon merolae	60%	6−7%
soybean (*Glycine max*)	100%	85−90%
barley (*Hordeum vulgare*)	61%	6−8%
wheat (*Triticum aestivum*)	47%	3−5%
Bacillus cereus	88%	0−3%
Bacillus flexus	95%	40%

[a]The activities of β-amylases are represented as residual activities. Data on the thermostability of β-amylase from other species were taken from the study by Sugita et al. (2011).[5]

maltose contributed little to improving the thermostability of the CmBAM protein (Figure 3). The K_m values were similar to plant-derived β-amylase (0.7−6.8), with some variation, except for β-amylase from *Abrus precatorius* (Table 1).

Sequence analyses suggest the characteristics of CmBAM. The SH reagent is a typical β-amylase inhibitor. Although the leucine residue at position 446 is not essential for the activity of β-amylase from soybean, modification of this residue has been shown to greatly reduce activity.[31] β-Amylases from plants and eukaryotic algae are distantly related to those from bacteria. Bacterial β-amylase has a raw starch-binding domain of approximately 100 amino acid residues in the N-terminal region,[34] but this domain is not present in β-amylases from red algae, green algae, and higher plants, including CmBAM. CmBAM possesses a unique inserted region that is not in other species, i.e., amino acid residues at positions 156 to 199 (second row in Figure 7). The 3D modeling reveals that this region is located outside and seems flexible (Figure S4). Further analysis is required to reveal the role of this inserted region in CmBAM. The results of the phylogenetic analysis of CmBAM were consistent with several reports that the set of carbohydrate-metabolizing enzymes possessed by red algae, green algae, and plants originated from a common eukaryotic ancestor and may have diverged early in the primitive plant Rhodophyta[26,35] (Figure 8).

The addition of Mg^{2+}, Ca^{2+}, and Zn^{2+} increases β-amylase activity,[36,37] while the addition of Mg^{2+}, Fe^{3+}, Cu^{2+}, and Zn^{2+} decreases β-amylase activity.[3,4,36,38] Zn^{2+} and Mg^{2+} increase or decrease the activity of β-amylase. However, in CmBAM, the changes with the addition of these metal ions were small, and no significant differences were observed when 1 or 10 mM $ZnSO_4$, $CaCl_2$, and $MgCl_2$ were added (Figure 2). Previous studies have shown that Fe^{3+} has a large inhibitory effect (residual activity of 0−1%) in some studies,[4,36] but it did not inhibit CmBAM (Figure 2). As per a previous report, these metal ions bind to the active site of β-amylases and either activate or competitively inhibit its activity as an auxiliary factor.[39] However, CmBAM is less sensitive to metal ions than the other β-amylases (Figure 2). The amino acid sequence around the active site of CmBAM was similar to that of other β-amylases, and the mechanism responsible for the difference in inhibition by metal ions is not yet clear. The report that Na^+ or K^+ also activates β-amylase was consistent with the present results (Figure 2). On the other hand, CmBAM was not activated by NaCl or KCl, suggesting that Cl^- may reduce CmBAM activity (Figure 2). In the case of higher plants, metal-tolerant amylase is beneficial for seed germination because soils are often polluted by heavy metals.[40] *Cyanidio-*

https://doi.org/10.1021/acsomega.2c03315
ACS Omega 2022, 7, 36195−36205

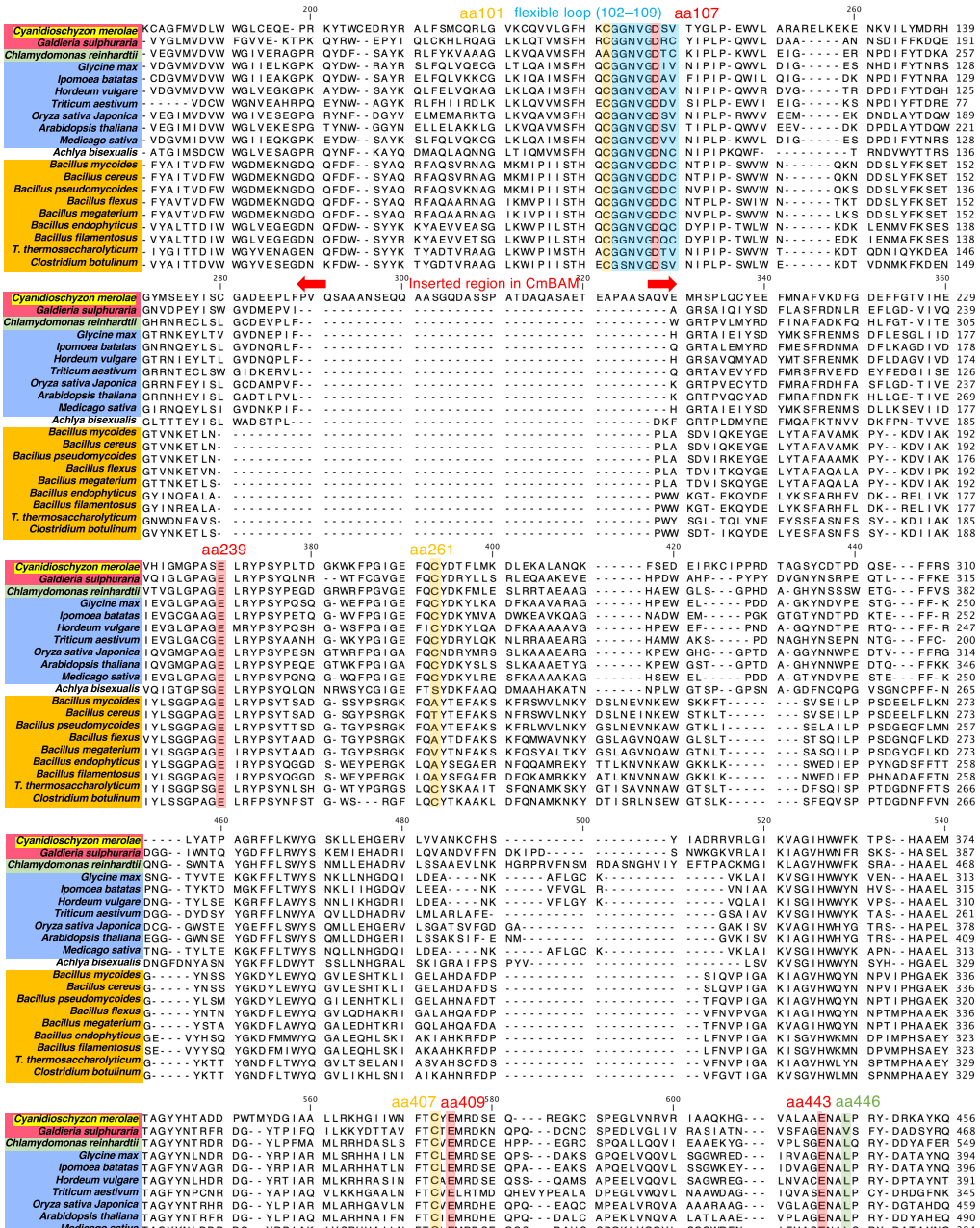

Figure 7. Comparison of amino acid sequences of 20 biochemically characterized β-amylases. Labels of each species from which each sequence was derived are shown in red: red algae, green: green algae, blue: higher plants, yellow: bacteria, and white: fungi. The amino acid residues essential for the expression of activity in the sequence, namely, the aspartic acid residue at position 107 (aa107) and the glutamic acid residues at positions 239, 409, and 443 (aa239, aa409, and aa443), are indicated in red. The flexible loop (aa102−109) consisting of amino acid residues 102−109 is shown in light blue; cysteine residues at positions 101 and 407 are targets of SH reagents; and cysteine residues at position 261, which is conserved only in the plant form (aa101, aa 407, and aa261), are shown in yellow. The leucine residue at position 446 (aa446) is shown in green. Amino acid numbers are based on the amino acid sequence of β-amylase from *C. merolae*. An inserted region only possessed by CmBAM is indicated by red arrows (aa156−199).

schyzon merolae cells live in an acidic hot spring, including many irons, and hence, the metal tolerance of CmBAM may be important for their survival under their environmental conditions.

The specificity of CmBAM for amylopectin and glycogen was similar to that of β-amylases from higher plants, but its substrate specificity for amylose was unique and higher than that of β-amylases from higher plants (Table 2). On the other hand, the specificities for amylose, amylopectin, and glycogen were different from those of β-amylases from *Bacillus flexus* and *C. thermosulphurogenes* (Table 2). Starch is composed of amylose and amylopectin, but the floridean starch synthesized

https://doi.org/10.1021/acsomega.2c03315
ACS Omega 2022, 7, 36195−36205

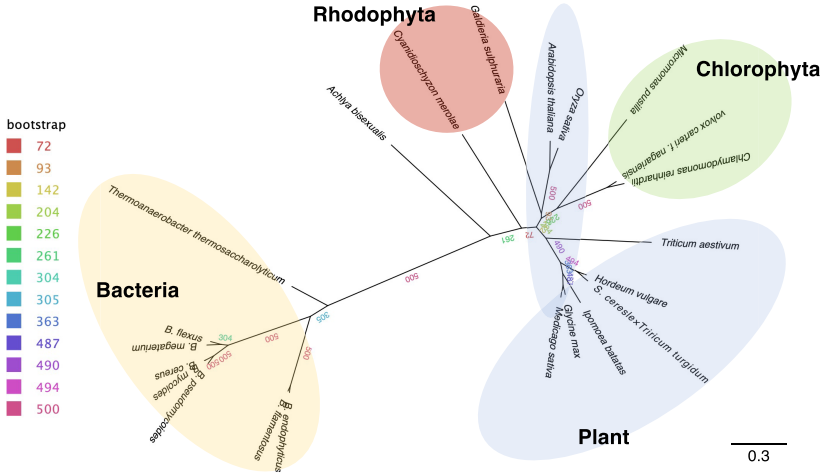

Figure 8. Phylogenetic analysis of β-amylases from various red algae, green algae, higher plants, and bacteria. Sequences of 22 β-amylases were obtained from GenBank. Sequence alignment of β-amylases was performed using CLC Sequence Viewer ver. 7.0. PhyML online was used to generate phylogenetic trees using the maximum likelihood method based on 289 conserved amino acid residues. The bootstrap value obtained by 500 replications indicates the reliability of each branch.

Table 5. Comparison of the Reusability and Storage Stability of Immobilized β-Amylases Using Other Carriers[a]

carriers	reusability (%)	storage stability (%)	reference
silica gel	81% (10 cycles)	89.6% (30 days)	
chitosan coated polyvinyl chloride(PVC) beads	72% (10 cycles)	55% (120 days)	53
polyvinylpyrrolidone (PVP) & chitosan blended beads	60% (10 cycles)	55% (120 days)	
$ZnFe_2O_4$ with SiO_2-NH_2	83% (6 cycles)	79.2% (12 days)	54
$Na_2MoO_4 \cdot 2H_2O$	80% (10 cycles)	83% (30 days)	8
iron oxide nanoparticles (Fe_3O_4)	80% (10 cycles)	93.4% (30 days)	9
graphene oxide nanosheets (GO)	50% (10 cycles)	97.6% (30 days)	
graphene oxide-carbon nanotube composite (GO-CNT)	70% (10 cycles)	75.4% (30 days)	

[a]The activity of β-amylases was represented as a residual activity, and the initial activity of the immobilized enzyme was set to 100%. Immobilized β-amylases from fenugreek (*Trigonella foenumgraecum*) or peanut (*Arachis hypogaea*) were used in the study by Srivastava et al. (2015)[53] and Das et al. (2017 or 2018),[8,9] respectively. The study by Rasouli et al. (2016)[54] did not show what organism the β-amylase was derived from.

by *C. merolae* as a storage glucan is composed of semi-amylopectin. The closely related *Cyanidium caldarium* and *G. sulphuraria* store glycogen in the cytoplasm as storage glucans.[41,42] A previous report showed that *C. merolae* has no amylose synthase (GBSS) and no amylose chain.[25,34] However, contrary to expectations, CmBAM had a higher substrate specificity for amylose than starch, glycogen, or amylopectin. The high specificity for amylose suggests that CmBAM cooperates with isoamylase and pullulanase *in vivo*. In addition, the high specificity for amylose supports the hypothesis of Deschamps et al. (2008) that *C. merolae* lost its ability to synthesize amylose with the loss of GBSS but that the common ancestor of Archaeplastida (including land plants, green algae, red algae, and glaucophytes) could synthesize both semiamylopectin and amylose.[26,27,35]

The immobilization efficiency of the enzyme was calculated to be 30−40% (Figure 4A). The amount of CmBAM remaining in the supernatant after immobilization was 62−71% of the amount of protein added, indicating that CmBAM activity remained active after immobilization (Figure 4B). The activity of the immobilized enzyme may be reduced by the physical constraints of the polymer, such as starch.[43] In addition, since the amino acid residues that bind to the carrier are random, there is a risk of inhibition of the active site. However, the immobilization of CmBAM on silica gel carriers did not suffer from the inhibition described above. Furthermore, the wider range of temperatures that can be used will lead to the expansion of applications and the improvement of the ease of handling CmBAM. Compared with several reported immobilized plant-derived β-amylases, immobilized CmBAM was comparable to β-amylase, with the highest reusability and the third-highest storage stability at 30 days (Table 5). The enzyme activity was 88% after incubation at 60 °C, indicating an improvement in thermostability at 15−20 °C (Figure 5). In the field of food production, it is important that the enzyme does not remain in the final product and that the carrier is safe.[44] Furthermore, since CmBAM was inhibited by the product maltose (Figure 2), the fact that the enzyme is not desorbed and can easily be separated from the product may be a great advantage. The enzyme activity remained nearly half after incubation at 70 °C (Figure 5), and further improvement of CmBAM immobilization active at 70 °C leads to the industrialization of this enzyme.

CONCLUSIONS

In this study, we clarified the biochemical and physical properties of CmBAM, but the specific role of CmBAM *in vivo* and its contribution to metabolism have not yet been clarified. The immobilization rate remains an issue. For practical use, the establishment of methods for mass cultivation of *C. merolae* cells and extraction of enzyme proteins, as well as cost and safety considerations, will be a future challenge. The significance *in vivo* also requires investigation of many complex

https://doi.org/10.1021/acsomega.2c03315
ACS Omega 2022, 7, 36195−36205

factors, such as the roles and expression of other isoamylases, glycogen phosphorylase, GWD, and DPE2 *in vivo* or *in vitro*; changes in starch metabolism related to circadian rhythm; and genes involved in the phosphorylation of glycogen phosphorylase and other enzymes.

■ ASSOCIATED CONTENT

Supporting Information

The Supporting Information is available free of charge at https://pubs.acs.org/doi/10.1021/acsomega.2c03315.

CmBAM enzymatic activity at the different substrate concentrations used for calculation in Table 1 (Figure S1); effect of GST-tag on CmBAM activity (Figure S2); relative activity of CmBAM for different amounts of the silica gel and different amounts of CmBAM added during immobilization (Figure S3); and 3D-modeling of CmBAM with the SWISS-Model server (Figure S4) (PDF)

■ AUTHOR INFORMATION

Corresponding Author

Takashi Osanai − *School of Agriculture, Meiji University, Kawasaki, Kanagawa 214-8571, Japan;* orcid.org/0000-0003-2229-6028; Phone: +81-44-934-7103; Email: tosanai@meiji.ac.jp; Fax: +81-44-934-7103

Author

Miyabi Murakami − *School of Agriculture, Meiji University, Kawasaki, Kanagawa 214-8571, Japan*

Complete contact information is available at: https://pubs.acs.org/10.1021/acsomega.2c03315

Author Contributions

M.M. designed the research, performed the experiments, analyzed the data, and wrote the manuscript. T.O. designed the research and wrote the manuscript.

Notes

The authors declare no competing financial interest.

■ ACKNOWLEDGMENTS

This work was supported by the Ministry of Education, Culture, Sports, Science, and Technology, Japan, by a grant to T.O. from JST-ALCA of the Japan Science and Technology Agency (grant JPMJAL1306), and by the JSPS KAKENHI Grant-in-Aid for Scientific Research (B) (grant 20H02905) and Grant-in-Aid for Challenging Research (Pioneering) (grant 20K21294).

■ ABBREVIATION

BAM β-amylase

■ REFERENCES

(1) Henrissat, B. A classification of glycosyl hydrolases based on amino acid sequence similarities. *Biochem. J.* **1991**, *280*, 309−316.

(2) Taniguchi, H.; Honda, Y.Amylase. *Encyclopedia of Microbiology, 3e.*, Academic Press, 2009, 159−173.

(3) Yamasaki, Y. Beta-amylase in germinating millet seeds. *Phytochemistry* **2003**, *64*, 935−939.

(4) Kocabay, S.; Cetinkaya, S.; Akkaya, B.; Yenidünya, A. F. Characterization of thermostable β-amylase isozymes from *Lactobacillus fermentum*. *Int. J. Biol. Macromol.* **2016**, *93*, 195−202.

(5) Sugita, A.; Okada, M.; Tani, A.; Minoda, M.; Yamaguchi, S. Thermostable β-amylase from *Bacillus flexus*. *J. Appl. Glycosci.* **2011**, *1*, 194−200.

(6) Garcia-Galan, C.; Berenguer-Murcia, Á.; Fernandez-Lafuente, R.; Rodrigues, R. C. Potential of different enzyme immobilization strategies to improve enzyme performance. *Adv. Synth. Catal.* **2011**, *353*, 2885−2904.

(7) Almulaiky, Y. Q.; El-Shishtawy, R. M.; Aldhahri, M.; Mohamed, S. A.; Afifi, M.; Abdulaal, W. H.; Mahyoub, J. A. Amidrazone modified acrylic fabric activated with cyanuric chloride: a novel and efficient support for horseradish peroxidase immobilization and phenol removal. *Int. J. Biol. Macromol.* **2019**, *140*, 949−958.

(8) Das, R.; Mishra, H.; Srivastava, A.; Kayastha, A. M. Covalent immobilization of β-amylase onto functionalized molybdenum sulfide nanosheets, its kinetics and stability studies: A gateway to boost enzyme application. *Chem. Eng. J.* **2017**, *328*, 215−227.

(9) Das, R.; Talat, M.; Srivastava, O. N.; Kayastha, A. M. Covalent immobilization of peanut β-amylase for producing industrial nanobiocatalysts: a comparative study of kinetics, stability and reusability of the immobilized enzyme. *Food Chem.* **2018**, *245*, 488−499.

(10) Kim, J.; Grate, J. W.; Wang, P. Nanostructures for enzyme stabilization. *Chem. Eng. Sci.* **2006**, *61*, 1017−1026.

(11) Livage, J.; Coradin, T.; Roux, C. Encapsulation of biomolecules in silica gels. *J. Phys.: Condens. Matter* **2001**, *13*, R673−R691.

(12) Cao, L.; Van Langen, L. M.; Van Rantwijk, F.; Sheldon, R. A. Cross-linked aggregates of penicillin acylase: robust catalysts for the synthesis of β-lactam antibiotics. *J. Mol. Catal. B: Enzym.* **2001**, *11*, 665−670.

(13) O'Fagain, C. Enzyme stabilization—recent experimental progress. *Enzyme Microb. Technol.* **2003**, *33*, 137−149.

(14) Kuroiwa, T. The primitive red algae *Cyanidium caldarium* and *Cyanidioschyzon merolae* as model system for investigating the dividing apparatus of mitochondria and plastids. *BioEssays* **1998**, *20*, 344−354.

(15) Matsuzaki, M.; Mitsumi, O.; Shin-I, T.; Maruyama, S.; Takahara, M.; Miyagishima, S. Y.; Mori, T.; Nishida, K.; Yagisawa, F.; Nishida, K.; Yoshida, Y.; Nishimura, Y.; Nakao, S.; Kobayashi, T.; Momoyama, Y.; Higashiyama, T.; Minoda, A.; Sano, M.; Nomoto, H.; Oishi, K.; Hayashi, H.; Ohta, F.; Nishizaka, S.; Haga, S.; Miura, S.; Morishita, T.; Kabeya, Y.; Terasawa, K.; Suzuki, Y.; Ishii, Y.; Asakawa, S.; Takano, H.; Ohta, N.; Kuroiwa, H.; Tanaka, K.; Shimizu, N.; Sugano, S.; Sato, N.; Nozaki, H.; Ogasawara, N.; Kohara, Y.; Kuroiwa, T. Genome sequence of the ultrasmall unicellular red alga *Cyanidioschyzon merolae* 10D. *Nature* **2004**, *428*, 653−657.

(16) Nozaki, H.; Takano, H.; Misumi, O.; Terasawa, K.; Matsuzaki, M.; Maruyama, S.; Nishida, K.; Yagisawa, F.; Yoshida, Y.; Fujiwara, T.; Takio, S. A 100%-complete sequence reveals unusually simple genomic features in the hot-spring red alga *Cyanidioschyzon merolae*. *BMC Biol.* **2007**, *5*, 28.

(17) Miyagishima, S. Y.; Itoh, R.; Toda, K.; Takahashi, H.; Kuroiwa, H.; Kuroiwa, T. Orderly formation of the double ring structures for plastid and mitochondrial division in the unicellular red alga *Cyanidioschyzon merolae*. *Planta* **1998**, *206*, 551−560.

(18) Nishida, K.; Yagisawa, F.; Kuroiwa, H.; Nagata, T.; Kuroiwa, T. Cell cycle-regulated, microtubule-independent organelle division in *Cyanidioschyzon merolae*. *Mol. Biol. Cell* **2005**, *16*, 2493−2502.

(19) Fukuda, S.; Hirasawa, E.; Takemura, T.; Takahashi, S.; Chokshi, K.; Pancha, I.; Tanaka, K.; Imamura, S. Accelerated triacylglycerol production without growth inhibition by overexpression of a glycerol-3-phosphate acyltransferase in the unicellular red alga *Cyanidioschyzon merolae*. *Sci. Rep.* **2018**, *8*, 1−12.

(20) Pancha, I.; Takaya, K.; Tanaka, K.; Imamura, S. The Unicellular red alga *Cyanidioschyzon merolae*, an excellent model organism for elucidating fundamental molecular mechanisms and their applications in biofuel production. *Plants* **2021**, *10*, 1218.

(21) Takusagawa, M.; Nakajima, Y.; Saito, T.; Misumi, O. Primitive red alga *Cyanidioschyzon merolae* accumulates storage glucan and triacylglycerol under nitrogen depletion. *J. Gen. Appl. Microbiol.* **2016**, *62*, 111−117.

(22) Ito, S.; Iwazumi, K.; Sukigara, H.; Osanai, T. Fumarase from *Cyanidioschyzon merolae* stably shows high catalytic activity for fumarate hydration under high temperature conditions. *Front. Microbiol.* **2020**, *11*, 2190.
(23) Osanai, T.; Iijima, H. Foods, heat treatment method of foods, manufacturing method of phycocyanin, manufacturing method of organic acid and manufacturing method of hydrogen. *Japanese Patent* **2017**, 2017−123816.
(24) Viola, R.; Nyvall, P.; Pedersén, M. The unique features of starch metabolism in red algae. *Proc. R. Soc. Lond. B.* **2001**, *268*, 1417−1422.
(25) Coppin, A.; Varré, J. S.; Lienard, L.; Dauvillée, D.; Guérardel, Y.; Soyer-Gobillard, M. O.; Buléon, A.; Ball, S.; Tomavo, S. Evolution of plant-like crystalline storage polysaccharide in the protozoan parasite *Toxoplasma gondii* argues for a red algal ancestry. *J. Mol. Evol.* **2005**, *60*, 257−267.
(26) Ball, S.; Colleoni, C.; Cenci, U.; Raj, J. N.; Tirtiaux, C. The evolution of glycogen and starch metabolism in eukaryotes gives molecular clues to understand the establishment of plastid endosymbiosis. *J. Exp. Bot.* **2011**, *62*, 1775−1801.
(27) Deschamps, P.; Haferkamp, I.; d'Hulst, C.; Neuhaus, H. E.; Ball, S. G. The relocation of starch metabolism to chloroplasts: when, why and how. *Trends Plant Sci.* **2008**, *13*, 574−582.
(28) Brizzee, C. O. (2021) Reversible glucan phosphorylation in the red alga, Cyanidioschyzon merolae. Ph.D. thesis, University of Kentucky, DOI: 10.13023/etd.2021.216
(29) Chia, T.; Thorneycroft, D.; Chapple, A.; Messerli, G.; Chen, J.; Zeeman, S. C.; Smith, S. M.; Smith, A. M. A cytosolic glucosyltransferase is required for conversion of starch to sucrose in *Arabidopsis* leaves at night. *Plant J.* **2004**, *37*, 853−863.
(30) Bernfield, P. Amylases α and β. *Meth. Enzymol.* **1955**, *1*, 149−158.
(31) Totsuka, A.; Fukazawa, C. Structure and function of soybean β-amylase. *J. Appl. Glycosci.* **1998**, *45*, 207−214.
(32) Zenvirth, D.; Volokita, M.; Kaplan, A. Photosynthesis and inorganic carbon accumulation in the acidophilic alga *Cyanidioschyzon merolae*. *Plant Physiol.* **1985**, *77*, 237−239.
(33) Kaplan, F.; Sung, D. Y.; Guy, C. L. Roles of β-amylase and starch breakdown during temperatures stress. *Physiol. Plant.* **2006**, *126*, 120−128.
(34) Saha, B. C.; Lecureux, L. W.; Zeikus, J. G. Raw starch adsorption-desorption purification of a thermostable β-amylase from *Clostridium thermosulfurogenes*. *Anal. Biochem.* **1988**, *175*, 569−572.
(35) Hirabaru, C.; Izumo, A.; Fujiwara, S.; Tadokoro, Y.; Shimonaga, T.; Konishi, M.; Yoshida, M.; Fujita, N.; Nakamura, Y.; Yoshida, M.; Kuroiwa, T.; Tsuzuki, M. The primitive rhodophyte *Cyanidioschyzon merolae* contains a semiamylopectin-type, but not an amylose-type, α-glucan. *Plant Cell Physiol.* **2010**, *51*, 682−693.
(36) Sagu, S. T.; Nso, E. J.; Homann, T.; Kapseu, C.; Rawel, H. M. Extraction and purification of beta-amylase from stems of *Abrus precatorius* by three phase partitioning. *Food Chem.* **2015**, *183*, 144−153.
(37) Shen, G. J.; Saha, B. C.; Lee, Y. E.; Bhatnagar, L.; Zeikus, J. G. Purification and characterization of a novel thermostable β-amylase from *Clostridium thermosulphurogenes*. *Biochem. J.* **1988**, *254*, 835−840.
(38) Hyun, H. H.; Zeikus, J. G. General biochemical characterization of thermostable pullulanase and glucoamylase from *Clostridium thermohydrosulfuricum*. *Appl. Environ. Microbiol.* **1985**, *49*, 1168−1173.
(39) Dahot, U. M.; Saboury, A. A.; Moosavi-Movahedi, A. A. Inhibition of β-amylase activity by calcium, magnesium and zinc ions determined by spectrophotometry and isothermal titration calorimetry. *J. Enzyme Inhib. Med. Chem.* **2004**, *19*, 157−160.
(40) Al-Hazmi, N. E.; Naguib, D. M. Amylase properties and its metal tolerance during rice germination improved by priming with rhizobacteria. *Rizosphere* **2022**, *22*, No. 100518.
(41) Martinez-Garcia, M.; Stuart, M. C.; van der Maarel, M. J. Characterization of the highly branched glycogen from the thermoacidophilic red microalga *Galdieria sulphuraria* and comparison with other glycogens. *Int. J. Biol. Macromol.* **2016**, *89*, 12−18.
(42) Shimonaga, T.; Konishi, M.; Oyama, Y.; Fujiwara, S.; Satoh, A.; Fujita, N.; Colleoni, C.; Buléon, A.; Putaux, J.; Ball, S. G.; Yokoyama, A.; Hara, Y.; Nakamura, Y.; Tsuzuki, M. Variation in storage α-glucans of the Porphyridiales (Rhodophyta). *Plant Cell Physiol.* **2008**, *49*, 103−116.
(43) Storey, K. B.; Schafhauser-Smith, D. Y. Immobilization of polysaccharide-degrading enzymes. *Biotechnol. Genet. Eng. Rev.* **1994**, *12*, 409−466.
(44) Das, R.; Kayastha, A. M. β-Amylase: General properties, mechanism and panorama of applications by immobilization on nanostructures. *Biocatalysis* **2019**, 17−38.
(45) Matsui, H.; Chiba, S.; Shimomura, T. Purification and some properties of active β-amylase in Rice. *Agr. Biol. Chem.* **1977**, *41*, 841−847.
(46) Kang, Y. N.; Tanabe, A.; Adachi, M.; Utsumi, S.; Mikami, B. Structural analysis of threonine 342 mutants of soybean β-amylase: role of a conformational change of the inner loop in the catalytic mechanism. *Biochemistry* **2005**, *44*, 5106−5116.
(47) Doehlert, D. C.; Duke, S. H.; Anderson, L. Beta-amylases from alfalfa (*Medicago sativa* L.) roots. *Plant Physiol.* **1982**, *69*, 1096−1102.
(48) Hirata, A.; Adachi, M.; Utsumi, S.; Mikami, B. Engineering of the pH optimum of *Bacillus cereus* β-amylase: conversion of the pH optimum from a bacterial type to a higher-plant type. *Biochemistry* **2004**, *43*, 12523−12531.
(49) Yoshigi, N.; Okada, Y.; Maeba, H.; Sahara, H.; Tamaki, T. Construction of a plasmid used for the expression of a sevenfold-mutant barley beta-amylase with increased thermostability in *Escherichia coli* and properties of the sevenfold-mutant beta-amylase. *J. Biochem.* **1995**, *118*, 562−567.
(50) Zhang, H.; Shen, W. B.; Zhang, W.; Xu, L. L. A rapid response of beta-amylase to nitric oxide but not gibberellin in wheat seeds during the early stage of germination. *Planta* **2005**, *220*, 708−716.
(51) Nanmori, T.; Shinke, R.; Aoki, K.; Nishira, H. Purification and characterization of β-amylase from *Bacillus cereus* BQ10-S1 Spo II. *Agr. Biol. Chem.* **1983**, *47*, 941−947.
(52) Lee, J. S.; Wittchen, K. D.; Stahl, C.; Strey, J.; Meinhardt, F. Cloning, expression, and carbon catabolite repression of the *bamM* gene encoding beta-amylase of *Bacillus megaterium* DSM319. *Appl. Microbiol. Biotechnol.* **2001**, *56*, 205−211.
(53) Srivastava, G.; Roy, S.; Kayastha, A. M. Immobilisation of Fenugreek β-amylase on chitosan/PVP blend and chitosan coated PVC beads: A comparative study. *Food Chem.* **2015**, *172*, 844−851.
(54) Rasouli, N.; Sohrabi, N.; Zamani, E. Influence of a novel magnetic recoverable support on kinetic, stability and activity of beta-amylase enzyme. *Phys. Chem. Res.* **2016**, *4*, 271−283.

https://doi.org/10.1021/acsomega.2c03315
ACS Omega 2022, 7, 36195−36205